

Memory-Efficient Pseudo-Labeling for Online Source-Free Universal Domain Adaptation using a Gaussian Mixture Model

Pascal Schlachter, Simon Wagner, Bin Yang

Institute of Signal Processing and System Theory, University of Stuttgart, Germany

{pascal.schlachter, bin.yang}@iss.uni-stuttgart.de

Abstract

In practice, domain shifts are likely to occur between training and test data, necessitating domain adaptation (DA) to adjust the pre-trained source model to the target domain. Recently, universal domain adaptation (UniDA) has gained attention for addressing the possibility of an additional category (label) shift between the source and target domain. This means new classes can appear in the target data, some source classes may no longer be present, or both at the same time. For practical applicability, UniDA methods must handle both source-free and online scenarios, enabling adaptation without access to the source data and performing batch-wise updates in parallel with prediction. In an online setting, preserving knowledge across batches is crucial. However, existing methods often require substantial memory, e.g. by using memory queues, which is impractical because memory is limited and valuable, in particular on embedded systems. Therefore, we consider memory-efficiency as an additional constraint in this paper. To achieve memory-efficient online source-free universal domain adaptation (SF-UniDA), we propose a novel method that continuously captures the distribution of known classes in the feature space using a Gaussian mixture model (GMM). This approach, combined with entropy-based out-of-distribution detection, allows for the generation of reliable pseudo-labels. Finally, we combine a contrastive loss with a KL divergence loss to perform the adaptation. Our approach not only achieves state-of-the-art results in all experiments on the DomainNet dataset but also significantly outperforms the existing methods on the challenging VisDA-C dataset, setting a new benchmark for online SF-UniDA. Our code is available at <https://github.com/pascalschlachter/GMM>.

1. Introduction

Despite the impressive results deep neural networks have demonstrated across various applications, they still struggle

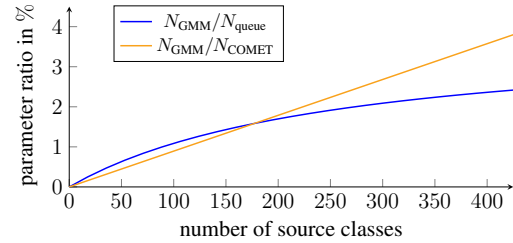


Figure 1. Comparison of the memory consumption between our GMM-based method, a memory queue modeled after [7], and an additional teacher model like used by COMET [37]. Our GMM-based method requires only a small fraction of the memory compared to the other two approaches.

when the training and test data $(x, y) \in \mathcal{X} \times \mathcal{Y}$ are not drawn i.i.d. from the same distribution \mathcal{P} on $\mathcal{X} \times \mathcal{Y}$ [33]. Here \mathcal{X} and \mathcal{Y} denote the input and label space, respectively. This issue arises when there is a domain (distribution) shift between the training and test data, a common problem in real-world applications. In this scenario, \mathcal{X} and \mathcal{Y} remain unchanged, but the distribution \mathcal{P}_t of the target domain differs from the distribution \mathcal{P}_s of the source domain. To tackle this challenge, unsupervised domain adaptation (UDA) is applied to adapt the pre-trained source model to the unlabeled target data. While classical UDA assumes the availability of the source dataset during adaptation, recent test-time adaptation (TTA) continuously adapts the pre-trained source model to the target domain(s) during deployment of the model using only the unlabeled test-time data. Accordingly, TTA is also known as source-free UDA. On one hand, being independent of the source dataset enables UDA even when the source data is inaccessible due to privacy concerns or memory constraints. On the other hand, by refraining to reprocess the source data during testing the computational efficiency is enhanced [39].

However, the vast majority of approaches towards TTA for classification only work in the standard closed-set setting, meaning they assume the source label space \mathcal{Y}_s to be identical to the target label space \mathcal{Y}_t . This greatly lim-

its the applicability for practical problems which are often open-world scenarios and therefore violate this assumption. To overcome this limitation and handle both a domain and a category (label) shift at the same time, source-free universal domain adaptation (SF-UniDA) [31] was introduced. Unlike previous approaches tailored to either partial-set DA (PDA), open-set DA (ODA) or open-partial-set DA (OPDA), SF-UniDA considers that usually no prior knowledge of the category shift is available. Thus, SF-UniDA aims to universally manage any kind of category shift.

In this way, SF-UniDA is related to few-shot learning [38] and class-incremental continual learning [42], both of which aim to enhance a pre-trained source model’s ability to accurately classify new classes using a small labeled target dataset. However, SF-UniDA differs in that it is unsupervised and thus does not rely on labeled target data. Consequently, in open-set or open-partial-set scenarios, SF-UniDA aims only to reject samples of new classes as unknown. Additionally, unlike few-shot learning and class-incremental continual learning, SF-UniDA addresses simultaneous domain and category shifts.

Besides category shifts, TTA was recently also extended to the online application. This advancement allows to adapt the source model continuously to the target data in parallel to inference, rather than relying on a fixed adaptation performed beforehand. Hence, each test batch is only accessed once and only one batch at a time. This is not only computationally more efficient but especially allows the application of TTA when, instead of a finite test set with unlimited access, real-time predictions for a data stream are required. Moreover, online TTA is versatile by being universally applicable to both online and offline scenarios.

Recently, [37] showed that most existing approaches towards SF-UniDA [30–32] do not generalize well to the online scenario since the individual batches cannot sufficiently represent their underlying data distribution. Therefore, approaches tackling this limitation aim to save the knowledge of previous batches either using a memory queue [7] or a mean teacher architecture [37]. However, both approaches require substantial memory which is a limited and valuable resource in practice.

Accordingly, in this paper, we introduce memory-efficiency as an additional constraint for online SF-UniDA, aiming to create a more realistic scenario and enhance applicability. Consequently, we propose a novel method designed to achieve memory-efficient online SF-UniDA. It uses a Gaussian mixture model (GMM) to adaptively capture the underlying distribution of the known classes in the target data within the feature space with only few parameters. In combination with an entropy-based out-of-distribution (OOD) detection, the GMM provides reliable pseudo-labels in the online scenario while remaining memory-efficient as shown in Fig. 1. Subsequently, for

adaptation, we apply a combination of a contrastive loss and a Kullback-Leibler (KL) divergence loss to get a meaningful feature space and clear predictions.

For evaluation, we test our GMM-based method on the two public DA datasets DomainNet and VisDA-C. Despite being strictly source-free and memory-efficient, it achieves state-of-the-art results across all evaluated domain and category shifts. Remarkably, on the VisDa-C dataset, our GMM-based method can even set a new state-of-the-art for online SF-UniDA by significantly outperforming all competing methods on all category shifts. This applies in particular to the OPDA scenario, where the margin to the second-best method is more than 13 %.

2. Related work

2.1. Online test-time adaptation

The goal of TTA is to adapt a standard pre-trained source model to the target domain. Thereby, unlike UDA, TTA does not require accessing the source data again during the adaptation process. In this paper, we focus on online TTA where the test data comes in as a stream of batches and therefore adaptation needs to happen in parallel to inference. Methods towards online TTA can be mainly classified into three categories. First, batch normalization (BN) statistics calibration methods [27, 39] adapt the BN layers of the source model to the shifted statistics of the target data. Second, self-training methods [7, 9, 12, 19] generate pseudo-labels for the target data to perform the adaptation in a supervised way. Third, entropy minimization methods [19, 26, 39] adapt the model such that the entropy of its outputs is minimized. However, all methods mentioned above do not consider the possibility of a category shift in addition to the domain shift.

2.2. Universal domain adaptation

Although numerous approaches address both domain and category shifts, most of them [1–6, 8, 11, 17, 22, 24, 25, 34–36, 40, 41] depend on access to source data. Additionally, some methods [15, 16, 20, 23] claim to be source-free because they do not reprocess the source data during adaptation, but they require a specialized, e.g. open-set, source model training and/or architecture. This reliance significantly limits their practical applicability. Following the strict definition given by [31], we do not consider these methods truly source-free since they depend on more source information than just a standard pre-trained source model. Among the remaining approaches, [10, 16, 18, 19] are not universal as they are either specialized for a single category shift or require prior knowledge about the type of shift.

The only approaches that are both truly source-free and universal are [30–32, 37], with [37] being the sole method additionally designed for the online setting. [31] introduces

a clustering-based pseudo-labeling for SF-UniDA called Global and Local Clustering (GLC). For adaptation, they combine a cross-entropy loss with a kNN-based loss. Finally, during inference, they apply an entropy threshold to reject samples of new classes as unknown. [32] extends this approach by a contrastive affinity learning strategy realized by an additional contrastive loss. [30] also builds on the work of [31] by using the same kNN-based loss and entropy-based rejection strategy for inference. However, they introduce a different pseudo-labeling approach called Learning Decomposition (LEAD) which divides features into source-known and -unknown components. This allows to build instance-level decision boundaries to identify target-private data during pseudo-labeling. For adaptation, they apply a confidence-weighted cross-entropy loss and a feature decomposition regularizer besides the kNN-based loss. Finally, [37] introduces a method called Contrastive Mean Teacher (COMET). It combines a contrastive and an entropy loss embedded into a mean teacher framework for pseudo-labeling. In this way, it is specially tailored to the online SF-UniDA scenario.

3. Method

3.1. Preliminaries

Our goal is to achieve universal DA in an online, source-free and memory-efficient manner. DA describes the task to adapt a neural network f , pre-trained on the source dataset $\mathcal{D}_s = \{\mathbf{x}_i^s \in \mathcal{X}_s, y_i^s \in \mathcal{Y}_s\}_{i=1}^{N_s}$, to the unlabeled target data $\mathcal{D}_t = \{\mathbf{x}_i^t \in \mathcal{X}_t, ? \in \mathcal{Y}_t\}_{i=1}^{N_t}$. The model can be divided into a feature extractor g and a classifier h , i.e. $f = h \circ g$. In contrast to conventional DA, universal DA considers the case that the target dataset \mathcal{D}_t experiences a category shift in addition to a domain shift. A category shift denotes the scenario that the target label space \mathcal{Y}_t deviates from the source label space \mathcal{Y}_s (i.e. $\mathcal{Y}_t \neq \mathcal{Y}_s$). This includes three cases: PDA ($\mathcal{Y}_t \subset \mathcal{Y}_s$), ODA ($\mathcal{Y}_s \subset \mathcal{Y}_t$) and OPDA ($\mathcal{Y}_s \cap \mathcal{Y}_t \neq \emptyset, \mathcal{Y}_s \not\subset \mathcal{Y}_t, \mathcal{Y}_s \not\supset \mathcal{Y}_t$). The goal of universal DA is to universally perform well in all three scenarios without any prior knowledge about the category shift. Obviously, this is the case if samples of new classes are reliably rejected as unknown while samples of known classes are classified correctly.

The paradigm source-free describes the constraint that the source dataset \mathcal{D}_s cannot be accessed during the adaptation. Hence, the standard pre-trained source model is the only source knowledge that can be leveraged. The second paradigm online denotes that the target data is not available as a dataset with unlimited access but instead is received as a stream of batches. This means that at any time we only have the current target batch $\{\mathbf{x}_{i,k}^t\}_{i=1}^{N_b}$ of size N_b for adaptation which demands an immediate prediction. Thereby, k represents the batch number. In this scenario, saving knowledge

from previously processed batches can be advantageous to improve the adaptation performance. Nevertheless, memory is limited and valuable in practice. Hence, the third paradigm we consider is to save this knowledge as memory-efficient as possible. By combining all three paradigms our proposed GMM-based approach features maximal applicability for real-world and especially embedded applications, where the source data is often subject to privacy policies, real-time inference of data streams may be required and hardware constraints must be met. Fig. 2 shows an overview of our method.

3.2. GMM-based pseudo-labeling

Self-training through pseudo-labeling is a well-established method that has proven to be successful for TTA [7, 9, 12, 19], SF-UniDA [30–32] and even online SF-UniDA [37]. Nevertheless, generating reliable pseudo-labels is particularly challenging in the online setting due to the limited amount of information available at any given time. Consequently, many pseudo-labeling techniques designed for offline use cannot be directly applied online. Clustering and kNN-based methods, in particular, perform poorly because individual target batches do not sufficiently represent the underlying data distribution [37].

To overcome this limitation, [7] proposed saving target samples into a memory queue to increase the amount of available data for pseudo-labeling. They show that in this way a kNN-based pseudo-labeling can be enabled. However, since their memory queue stores the features and predicted probabilities of 55388 samples it massively increases the memory requirement. A similar issue arises with [37], which requires a copy of the model to build a mean teacher framework. Depending on the applied architecture, this can also demand a substantial amount of memory.

While saving knowledge of previously processed target batches is essential to get well-founded pseudo-labels, this knowledge transfer must be as memory-efficient as possible. Otherwise, the practical applicability is limited since hardware constraints are easily violated. Therefore, we propose a novel method that achieves memory-efficient knowledge transfer resulting in a reliable pseudo-labeling for online SF-UniDA. Our basic idea is to continuously save the data distribution of the target data in the feature space using a GMM. Concretely, each of the $|\mathcal{Y}_s|$ known classes is modeled by a Gaussian distribution, representing a mode of the GMM. Although, the underlying assumption that each class follows a unimodal Gaussian distribution in the feature space cannot be guaranteed, the contrastive loss introduced in Sec. 3.4 supports this hypothesis by enforcing the class-wise clustering of samples in the feature space.

For each target batch $\{\mathbf{x}_{i,k}^t\}_{i=1}^{N_b}$ we first update the GMM parameters $\hat{\boldsymbol{\mu}}_k(c)$ and $\hat{\boldsymbol{\Sigma}}_k(c)$, i.e. the means and covariance matrices of all modes $1 \leq c \leq |\mathcal{Y}_s|$, by a weighted re-

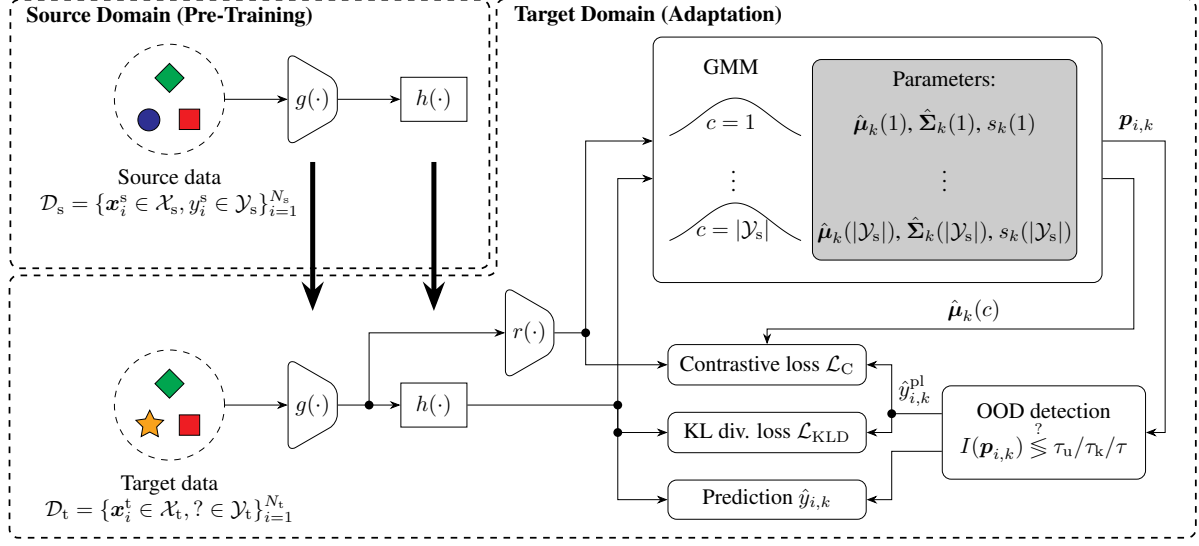


Figure 2. Overview of our proposed GMM-based approach for memory-efficient online SF-UniDA. After pre-training on the source data \mathcal{D}_s , the model is adapted to the target data \mathcal{D}_t using a combination of a contrastive loss \mathcal{L}_C and a KL divergence loss \mathcal{L}_{KLD} . For these losses, reliable pseudo-labels are provided by a GMM that models the distribution of the samples from the $|\mathcal{Y}_s|$ known classes in a reduced feature space. Its parameters are iteratively updated with each target batch. To reject samples from new classes as unknown during both pseudo-labeling and prediction, we apply an entropy-based OOD detection.

calculation inspired by the expectation maximization (EM) algorithm. Subsequently, the resulting GMM enables the calculation of the likelihood $p(\mathbf{x}_{i,k}^t | c; \hat{\boldsymbol{\mu}}_k(c), \hat{\boldsymbol{\Sigma}}_k(c))$ for a given target sample $\mathbf{x}_{i,k}^t$ belonging to class c , thus allowing us to generate reliable pseudo-labels.

The EM algorithm is divided into an E-step and an M-step. In the E-step, the weights are calculated. There are two types of weightings to consider. The first weighting determines how much each sample $\mathbf{x}_{i,k}^t$ within a single target batch $\{\mathbf{x}_{i,k}^t\}_{i=1}^{N_b}$ contributes to the update of each GMM parameter. Instead of deriving these weights from the GMM, we use the model predictions $f(\mathbf{x}_{i,k}^t)$. Second, weighting across batches accounts for the unequal representation of classes in different batches. A batch with more samples of a certain class should contribute more to the parameter update of that class than a batch with fewer samples. We achieve this by using the class-wise sum of all softmax classifier outputs of a batch as an indicator of class representation. By iteratively summing these values and comparing them to the current value, we determine how much the current batch should contribute to the overall parameter value. Accordingly, we define

$$s_k(c) = s_{k-1}(c) + \sum_{i=1}^{N_b} f_c(\mathbf{x}_{i,k}^t), \quad (1)$$

which is initialized by $s_0(c) = 0 \forall c$. Thereby, $f_c()$ denotes the softmax classifier output corresponding to class c .

In the following M-step, we recursively update both

the mean vector $\hat{\boldsymbol{\mu}}_k(c)$ and covariance matrix $\hat{\boldsymbol{\Sigma}}_k(c)$ for each mode c using the samples of the current target batch $\{\mathbf{x}_{i,k}^t\}_{i=1}^{N_b}$:

$$\hat{\boldsymbol{\mu}}_k(c) = \frac{s_{k-1}(c) \cdot \hat{\boldsymbol{\mu}}_{k-1}(c) + \sum_{i=1}^{N_b} f_c(\mathbf{x}_{i,k}^t) \cdot r_{i,k}}{s_k(c)} \quad (2)$$

$$\hat{\boldsymbol{\Sigma}}_k(c) = \frac{\left(s_{k-1}(c) \cdot \hat{\boldsymbol{\Sigma}}_{k-1}(c) + \sum_{i=1}^{N_b} f_c(\mathbf{x}_{i,k}^t) \cdot \left(r_{i,k} - \hat{\boldsymbol{\mu}}_k(c) \right) \left(r_{i,k} - \hat{\boldsymbol{\mu}}_k(c) \right)^T \right)}{s_k(c)} \quad (3)$$

Thereby, $r_{i,k}$ is an abbreviation for $r(g(\mathbf{x}_{i,k}^t))$ where $r()$ denotes a feature dimension reduction function. We found that applying our GMM-based pseudo-labeling in a lower-dimensional feature space than the output of $g()$ not only reduces the memory requirement of the GMM parameters but also improves performance. The dimension reduction is realized using a single linear layer, which is optimized in parallel to the model f .

Despite the iterative calculation, we do not require initialization of $\hat{\boldsymbol{\mu}}_0(c)$ and $\hat{\boldsymbol{\Sigma}}_0(c)$ since we initialize $s_0(c) = 0 \forall c$. Nevertheless, if prior knowledge is available, it can be incorporated by setting $\hat{\boldsymbol{\mu}}_0(c)$ and $\hat{\boldsymbol{\Sigma}}_0(c)$ accordingly and selecting appropriate weights $s_0(c)$.

After updating the GMM parameters, for each sample $\mathbf{x}_{i,k}^t$ in the current target batch $\{\mathbf{x}_{i,k}^t\}_{i=1}^{N_b}$ we determine the

likelihood $p(\mathbf{x}_{i,k}^t | c; \hat{\boldsymbol{\mu}}_k(c), \hat{\boldsymbol{\Sigma}}_k(c))$ across all known classes $1 \leq c \leq |\mathcal{Y}_s|$. This is done by evaluating each sample $\mathbf{x}_{i,k}^t$ on all $|\mathcal{Y}_s|$ Gaussian distributions $\mathcal{N}(\hat{\boldsymbol{\mu}}_k(c), \hat{\boldsymbol{\Sigma}}_k(c))$. In a standard closed-set scenario, pseudo-labels could directly be assigned based on the class with the maximum likelihood. However, since our goal is to address online SF-UniDA, an additional OOD detection is necessary to identify samples of new classes and pseudo-label them as unknown as described in the following section.

Finally, in Eq. (2) and Eq. (3), note that each sample contributes to all parameters. In this way, predictions of the GMM are also influenced by similar samples, leading to a reduction of noise in the pseudo-labels.

3.3. Out-of-distribution detection

Since the GMM only models known classes, a maximum likelihood (ML) estimation alone would classify all samples as belonging to one of these known classes. However, for online SF-UniDA, it is crucial to identify samples from new classes and pseudo-label them accordingly by introducing a new ‘‘unknown’’ class $|\mathcal{Y}_s| + 1$. Therefore, we extend the GMM-based ML estimation with an OOD detection mechanism. We accomplish OOD detection by assessing the confidence of a sample belonging to the GMM distribution. Through empirical investigation, we determined that the normalized Shannon entropy of the likelihoods output by the GMM is most effective for this purpose. This entropy measure is defined as

$$I(\mathbf{p}_{i,k}) = -\frac{1}{\log |\mathcal{Y}_s|} \cdot \mathbf{p}_{i,k}^T \cdot \log \mathbf{p}_{i,k} \quad (4)$$

where $\mathbf{p}_{i,k} = \left[p(\mathbf{x}_{i,k}^t | c; \hat{\boldsymbol{\mu}}_k(c), \hat{\boldsymbol{\Sigma}}_k(c)) \right]_{c=1}^{|\mathcal{Y}_s|}$ represents a vector containing the likelihoods indicating the probability of sample $\mathbf{x}_{i,k}^t$ belonging to all classes $1 \leq c \leq |\mathcal{Y}_s|$. A low entropy value suggests high confidence that the sample $\mathbf{x}_{i,k}^t$ belongs to the GMM distribution, hence to one of the known classes. Conversely, a high entropy indicates low confidence that the sample belongs to this distribution, suggesting it is likely OOD and belongs to a new class.

Recently, [10] and [37] proposed excluding samples with uncertain pseudo-labels from the adaptation process. The intuition behind this approach is that incorrect pseudo-labels can lead to negative consequences, which are more harmful than using fewer samples for adaptation. In essence, prioritizing the quality of pseudo-labels over maximizing the quantity of samples used in adaptation is beneficial. We align with this perspective and therefore adopt a similar strategy. Instead of using a single entropy threshold to distinguish samples from new classes and known classes, we introduce two thresholds, τ_k and τ_u ($\tau_k < \tau_u$), to filter out samples with uncertain estimates and not assigning them a pseudo-label. The final pseudo-labeling of a target

sample $\mathbf{x}_{i,k}^t$ is described as follows:

$$\hat{y}_{i,k}^{\text{pl}} = \begin{cases} \arg \max_{c \in \mathcal{Y}_s} \mathbf{p}_{i,k} & I(\mathbf{p}_{i,k}) \leq \tau_k \\ |\mathcal{Y}_s| + 1 & I(\mathbf{p}_{i,k}) \geq \tau_u \\ \text{None} & \text{otherwise} \end{cases} \quad (5)$$

To avoid the unintuitive manual selection of the thresholds τ_k and τ_u , we adaptively initialize them on the fly within the first $N_{\text{init}} = 30$ batches. Thereby, for each of these batches, we sort the samples w.r.t. $I(\mathbf{p}_{i,k})$ and identify the entropy values that separate the top and bottom $(100 - p_{\text{reject}})/2$ percent of samples. We then calculate τ_k and τ_u by averaging these entropy values across the previously processed batches. After this initialization period, the thresholds remain fixed for the rest of the adaptation process. In this way, only p_{reject} and N_{init} need to be chosen manually, which are both well-interpretable for humans in contrast to τ_k and τ_u .

3.4. Contrastive loss

With the pseudo-labels output by our GMM-based method, we apply a contrastive loss [14] to perform the domain adaptation. It is able to enforce desired properties on the feature space by minimizing the distances of so-called positive pairs of samples and maximizing the distances of negative pairs. [18] and [37] have already proved that it can be successfully applied for online SF-UniDA. Following their idea, we want to enforce the samples of known classes to build dense and clearly separated clusters in the feature space. Moreover, the samples of new classes should be well-separated from these clusters. The contrastive loss achieves this by treating the combinations of each sample of a known class with both the other samples of the same class and the mean of the corresponding GMM mode as positive pairs. Regarding the negative pairs, for each sample of a known class, we maximize the distances to all samples of the different classes, including the ‘‘unknown’’ class. Moreover, we maximize the distances between each sample and the GMM’s means of all other classes.

Thereby, we extend each batch by adding one augmented version of each sample which not only doubles the number of samples used for adaptation but also leads to a consistent feature space being robust to small changes in the input.

Mathematically, the contrastive loss for the k -th target batch $\{\mathbf{x}_{i,k}^t\}_{i=1}^{N_b}$ is given as

$$\mathcal{L}_C = -\sum_{j=1}^{2N_b} \sum_{i=1}^{2N_b} \mathbb{1}(\hat{y}_{j,k}^{\text{pl}} = \hat{y}_{i,k}^{\text{pl}}) \log \frac{\exp\left(\frac{\langle \tilde{\mathbf{r}}_{j,k}, \tilde{\mathbf{r}}_{i,k} \rangle}{\tau}\right)}{\sum_{l=1}^{2N_b} \exp\left(\frac{\langle \tilde{\mathbf{r}}_{l,k}, \tilde{\mathbf{r}}_{i,k} \rangle}{\tau}\right)} \\ - \sum_{c=1}^{|\mathcal{Y}_s|} \sum_{i=1}^{2N_b} \mathbb{1}(\hat{y}_{i,k}^{\text{pl}} = c) \log \frac{\exp\left(\frac{\langle \hat{\boldsymbol{\mu}}_k(c), \tilde{\mathbf{r}}_{i,k} \rangle}{\tau}\right)}{\sum_{l=1}^{2N_b} \exp\left(\frac{\langle \hat{\boldsymbol{\mu}}_k(c), \tilde{\mathbf{r}}_{l,k} \rangle}{\tau}\right)} \quad (6)$$

where $\mathbb{1}(\cdot)$ denotes the indicator function, $\langle \cdot \rangle$ represents the cosine similarity, and τ is the temperature. Moreover, $\tilde{r}_{i,k}$ is an abbreviation for $r(g(\tilde{\mathbf{x}}_{i,k}^t))$, whereby $\{\tilde{\mathbf{x}}_{i,k}^t\}_{i=1}^{2N_b} = \{\mathbf{x}_{i,k}^t\}_{i=1}^{N_b} \cup \{\tilde{\mathbf{x}}_{i,k}^t\}_{i=1}^{N_b}$ denotes the union of the target batch $\{\mathbf{x}_{i,k}^t\}_{i=1}^{N_b}$ and its augmentation $\{\tilde{\mathbf{x}}_{i,k}^t\}_{i=1}^{N_b}$.

Note that OWTTC [18] and COMET-P [37] use source prototypes, i.e. the class-wise means of the feature representations of the source data, to serve as cluster centers for the contrastive loss. However, the availability of such source prototypes cannot be guaranteed in a source-free setting. In contrast, in our proposed GMM-based method, the cluster centers are given by the means of the individual modes of the GMM. Accordingly, no source prototypes are required which is a significant advantage.

3.5. KL divergence loss

While the contrastive loss only optimizes the feature extractor g to get the desired feature space, we combine it with a second loss to additionally optimize the translation between features and predictions performed by the classifier h . Thereby, it especially must be taught how to deal with samples of new classes, i.e. feature representations outside of the clusters of known classes, because this is not part of the closed-set source training. Concretely, to support our entropy-based OOD-detection, the goal is to enforce a small entropy for samples of the known classes and a large entropy for samples of new classes. We achieve this using the following KL divergence loss:

$$\begin{aligned} \mathcal{L}_{\text{KLD}} = & - \sum_{i=1}^{N_b} \mathbb{1}(\hat{y}_{i,k}^{\text{pl}} \in |\mathcal{Y}_s|) D_{\text{KL}}(\mathbf{u} \| f(\mathbf{x}_{i,k}^t)) \\ & + \sum_{i=1}^{N_b} \mathbb{1}(\hat{y}_{i,k}^{\text{pl}} \notin |\mathcal{Y}_s|) D_{\text{KL}}(\mathbf{u} \| f(\mathbf{x}_{i,k}^t)) \end{aligned} \quad (7)$$

where

$$D_{\text{KL}}(p \| q) = - \sum_i p_i \log q_i + \sum_i p_i \log p_i \quad (8)$$

denotes the KL divergence between two distributions p and q . $\mathbf{u} = \left[\frac{1}{|\mathcal{Y}_s|}, \dots, \frac{1}{|\mathcal{Y}_s|} \right]^T \in \mathbb{R}^{|\mathcal{Y}_s|}$ serves as a uniform reference distribution. Hence, the loss maximizes the KL divergence between the classifier output and the uniform distribution for samples pseudo-labeled as a known class and minimizes it for samples pseudo-labeled as unknown.

Finally, the overall loss is a combination of the contrastive and KL divergence loss, weighted by $\lambda > 0$:

$$\mathcal{L} = \mathcal{L}_C + \lambda \mathcal{L}_{\text{KLD}} \quad (9)$$

3.6. Inference

For inference, we combine standard prediction based on the maximum classifier output with the same OOD detection method used for pseudo-labeling. The only difference

is that we now use a single threshold, τ , because every sample must receive a prediction. We set τ as the average of the two thresholds from pseudo-labeling: $\tau = \frac{\tau_k + \tau_u}{2}$. The resulting prediction process for any sample $\mathbf{x}_{i,k}^t$ is as follows:

$$\hat{y}_{i,k} = \begin{cases} \arg \max f(\mathbf{x}_{i,k}^t) & I(\mathbf{p}_{i,k}) \leq \tau \\ |\mathcal{Y}_s| + 1 & I(\mathbf{p}_{i,k}) > \tau \end{cases} \quad (10)$$

3.7. Memory consumption

Eventually, we analyze the memory consumption of our GMM-based method and compare it to a memory queue modeled after [7] and using a mean teacher approach as proposed by [37]. For each mode, the GMM needs to store a mean vector $\hat{\boldsymbol{\mu}}_k(c)$, a covariance matrix $\hat{\boldsymbol{\Sigma}}_k(c)$, and a weight $s_k(c)$. The sizes of $\hat{\boldsymbol{\mu}}_k(c)$ and $\hat{\boldsymbol{\Sigma}}_k(c)$ are determined by the number of dimensions FD_r in the reduced feature space. Since covariance matrices are symmetric, $\hat{\boldsymbol{\Sigma}}_k(c)$ is fully defined by its upper or lower triangle, including the diagonal. As a result, the total number of values that need to be stored for the GMM is given by:

$$N_{\text{GMM}} = \left(FD_r + \frac{FD_r \cdot (FD_r + 1)}{2} + 1 \right) \cdot |\mathcal{Y}_s| \quad (11)$$

A memory queue like proposed by [7] stores both the features and classifier outputs of samples. Thus, the total number of values stored is given by:

$$N_{\text{queue}} = L \cdot (FD + |\mathcal{Y}_s|) \quad (12)$$

where L denotes the length of the queue, chosen to be $L = 55388$ in [7], and FD is the number of dimensions in the original feature space.

Using a mean teacher approach like COMET [37] requires maintaining a copy of the model, so the memory consumption depends on the model architecture and its number of parameters. The ResNet-50-based architecture used in the following experiments has approximately $N_{\text{COMET}} \approx 24,000,000$ parameters.

For a fair comparison of the three approaches, we use the same hyperparameters as in the subsequent experiments, i.e. $FD = 256$ and $FD_r = 64$. Fig. 1 shows the resulting plots of the ratios $N_{\text{GMM}}/N_{\text{queue}}$ and $N_{\text{GMM}}/N_{\text{COMET}}$ against the number of source classes $|\mathcal{Y}_s|$. It is evident that our GMM-based method requires only a small fraction of the memory compared to both other approaches. Specifically, even for $|\mathcal{Y}_s| = 345$ source classes (PDA scenario on the DomainNet dataset), the GMM based approach requires only approximately 2.2% of the memory needed by the memory queue and 3.1% compared to the mean teacher. This substantial reduction in memory usage makes the GMM-based approach better suited for embedded applications where memory resources are limited.

Table 1. Class splits, i.e. number of the shared, source-private and target-private classes, for OPDA, ODA and PDA, respectively

	$ \mathcal{Y}_s \cap \mathcal{Y}_t , \mathcal{Y}_s \setminus \mathcal{Y}_t , \mathcal{Y}_t \setminus \mathcal{Y}_s $		
	PDA	ODA	OPDA
DomainNet	200, 145, 0	200, 0, 145	150, 50, 145
VisDA-C	6, 6, 0	6, 0, 6	6, 3, 3

4. Experiments

4.1. Setup

To enable a fair comparison, we mainly follow the same experimental setup as [37]. Accordingly, in contrast to continual TTA, we only consider a single domain shift between the source and target domain. Due to space limitations, the results of thorough ablation studies providing deep insights into our method can be found in the supplementary material.

Datasets: To evaluate our GMM-based method, we utilize the two public DA datasets DomainNet [28] and VisDA-C [29]. From the DomainNet dataset, we use four domains: clipart (C), painting (P), real (R), and sketch (S). Each domain contains between approx. 48,000 and 173,000 images, distributed across 345 classes. The VisDA-C (V) dataset consists of 12 classes and only one domain shift from renderings of 3D models to real-world images from the Microsoft COCO dataset [21]. As intended, we use the first as the source domain having 152,397 images and the latter as target domain with 55,388 images.

To construct the category shifts, we take the first $|\mathcal{Y}_s|$ of the alphabetically ordered classes for source training and the last $|\mathcal{Y}_t|$ for the target domain. Obviously, the overlapping $|\mathcal{Y}_s \cap \mathcal{Y}_t|$ classes are shared between both domains. The class splits we used to create the three category shifts for each of the two datasets are given in Tab. 1.

Competing methods: Obviously, using source information or performing the adaptation offline before inference leads naturally to better results. Hence, we evaluate all methods in the same source-free and online setting to enable a fair comparison.

First, as a lower bound all methods need to surpass, we apply the source model without any adaptation and use an entropy threshold to enable the rejection of samples as unknown. Second, we use GLC [31], GLC++ [32] and LEAD [30] as competing methods. They are all intended for offline SF-UniDA but we simply apply them batch-wise in the online scenario. Third, we use OWTTT [18]. Although being originally designed to identify strong OOD data (e.g. samples of different datasets or random noise) in online TTA, [37] showed that it also performs well in online SF-

UniDA. Finally, we apply both versions of COMET [37], COMET-P and COMET-F, as the only existing method being specifically designed for online SF-UniDA.

Note that OWTTT [18] and COMET-P [37] use source prototypes. It is a matter of definition whether this is still considered source-free but it certainly limits their applicability in real-world applications.

Implementation details: To ensure a fair comparison, we use the same pre-trained source model for all methods. It is based on a ResNet-50 [13] architecture with a 256-dimensional feature space trained in a similar way like for [19], [31], and [37]. For adaptation, we apply a SGD optimizer with momentum 0.9 and a learning rate of 0.01 for VisDa-C and 0.001 for DomainNet. Moreover, we choose the batch size to $N_b = 64$. Regarding the hyperparameters of our GMM-based approach, we decide to reduce the number of features to $FD_r = 64$. Furthermore, regarding the OOD detection, we choose the ratio of samples left out during initialization of τ_k and τ_u to $p_{\text{reject}} = 50\%$ and the number of batches used for initialization to $N_{\text{init}} = 30$. Finally, we select the temperature for the contrastive loss to $\tau = 0.1$ and use $\lambda = 1$ to weigh both losses equally.

As customary, we provide the H-score, i.e. the harmonic mean of the accuracy of samples of known and new classes, for ODA and OPDA. For PDA, we use the standard classification accuracy. We perform each experiment six times and report the mean, respectively.

4.2. Results

The results are shown in Tab. 2. As expected, both GLC and GLC++ perform poorly in the online setting since they rely heavily on clustering and kNN. While LEAD performs significantly better than GLC and GLC++, it still underperforms the source-only results in nearly all experiments. In contrast, OWTTT shows a slight improvement over the source-only results for DomainNet in the ODA and OPDA scenarios, and it delivers remarkable performance on VisDA-C. However, this improvement does not extend to PDA, where OWTTT performs worse than the source-only approach on average for DomainNet. It is important to note that, although PDA may seem straightforward, it is challenging in the context of UniDA, as it is crucial to minimize the number of samples incorrectly rejected as unknown.

COMET-P and our GMM-based method perform similarly well on DomainNet, with their average results differing by less than 0.7%, 0.6%, and 0.1%, respectively. Both methods significantly improve the source-only performance. While COMET-F’s results are slightly lower compared to COMET-P and our GMM-based approach, it still outperforms the other methods, including the source-only baseline. These results of our GMM-based method are already notable because, unlike OWTTT and COMET-P,

Table 2. Results of the experiments. The best result is marked in red and the second best in blue, respectively.

(a) Accuracy in % for the PDA scenario														
PDA	C2P	C2R	C2S	P2C	P2R	P2S	R2C	R2P	R2S	S2C	S2P	S2R	Avg.	V
Source-only	17.5	31.3	21.0	25.0	41.5	24.0	34.1	30.5	22.7	24.7	17.8	25.2	26.28	17.1
OWTTT [18]	22.6	28.9	25.1	26.3	28.3	24.6	27.2	26.6	22.9	27.6	19.9	14.5	24.54	28.1
COMET-P [37]	24.8	41.2	30.3	34.5	51.3	35.8	40.6	36.1	30.6	37.5	30.6	41.1	36.20	32.1
GLC [31]	1.1	0.9	1.4	1.6	0.7	1.1	0.9	0.5	0.6	2.1	1.1	0.6	1.05	15.5
GLC++ [32]	0.1	0.1	0.2	0.2	0.1	0.2	0.1	0.1	0.1	0.3	0.1	0.1	0.14	1.2
LEAD [30]	6.8	6.2	10.5	13.4	6.9	10.5	9.2	5.5	4.9	18.2	9.0	5.9	8.92	14.4
COMET-F [37]	23.4	38.8	28.3	32.2	48.9	33.7	40.4	36.5	30.7	34.8	28.0	38.3	34.50	31.7
GMM (Ours)	27.9	39.7	32.4	34.6	43.7	33.8	43.2	39.5	33.4	41.3	34.3	38.9	36.89	40.9

(b) H-score in % for the ODA scenario														
ODA	C2P	C2R	C2S	P2C	P2R	P2S	R2C	R2P	R2S	S2C	S2P	S2R	Avg.	V
Source-only	36.3	51.3	39.9	41.2	57.8	40.4	50.2	47.0	38.4	44.4	30.7	45.9	43.63	31.7
OWTTT [18]	42.1	41.9	45.0	45.3	47.0	42.9	48.7	35.9	40.8	51.9	45.4	44.1	44.25	56.7
COMET-P [37]	42.4	54.8	46.8	47.9	57.2	47.7	53.8	50.8	46.3	52.7	39.0	52.7	49.34	50.9
GLC [31]	2.4	2.0	2.2	2.1	1.7	1.5	1.3	0.9	0.7	3.4	2.3	1.6	1.84	0.1
GLC++ [32]	0.2	0.2	0.3	0.2	0.1	0.2	0.1	0.1	0.1	0.4	0.2	0.1	0.18	0.1
LEAD [30]	30.9	38.6	36.5	34.0	36.6	30.8	33.3	27.6	23.2	44.5	33.7	36.3	33.83	19.7
COMET-F [37]	40.7	53.2	45.0	46.2	57.2	46.2	53.0	50.3	45.3	50.0	37.0	51.3	47.95	49.0
GMM (Ours)	42.7	53.9	46.3	46.8	55.5	43.7	50.7	49.8	44.1	52.3	45.2	54.1	48.76	59.7

(c) H-score in % for the OPDA scenario														
OPDA	C2P	C2R	C2S	P2C	P2R	P2S	R2C	R2P	R2S	S2C	S2P	S2R	Avg.	V
Source-only	39.5	55.4	42.7	42.0	57.6	38.8	51.7	47.6	38.6	46.8	32.2	47.9	45.07	26.9
OWTTT [18]	45.3	49.5	46.9	47.0	45.9	43.9	49.3	40.5	41.0	52.3	46.4	36.6	45.38	46.8
COMET-P [37]	45.6	58.6	48.9	47.8	57.7	46.8	55.5	51.5	46.2	54.1	39.0	54.2	50.49	42.9
GLC [31]	3.1	3.0	2.5	3.4	1.9	2.1	1.8	1.4	0.9	4.3	2.6	2.3	2.44	17.0
GLC++ [32]	0.3	0.2	0.4	0.3	0.1	0.2	0.2	0.1	0.1	0.4	0.3	0.1	0.22	0.5
LEAD [30]	33.3	42.0	37.4	35.0	37.4	31.1	33.5	30.1	25.2	45.6	34.9	37.9	35.28	23.8
COMET-F [37]	44.1	57.1	47.0	47.7	57.9	45.5	54.8	51.3	45.4	51.7	37.4	53.1	49.42	42.0
GMM (Ours)	45.6	57.4	48.1	48.5	57.1	43.9	52.2	50.9	44.9	53.8	46.4	56.1	50.41	60.3

our method is strictly source-free by not relying on source prototypes, and it requires significantly less memory than COMET-P and COMET-F. Even more impressive is the performance of our GMM-based approach on the VisDA-C dataset, where it clearly outperforms all other methods for all three category shifts. In the OPDA scenario, the margin to the second best method, OWTTT, is more than 13%.

5. Conclusion

Despite its practical importance, we identified memory-efficiency as a so-far overlooked aspect in SF-UniDA, particularly in online SF-UniDA. To address this limitation,

we proposed a novel approach that continuously captures the underlying distribution of the target data using a GMM. By enabling memory-efficient knowledge transfer across batches in the online scenario, this allows a reliable pseudo-labeling. Concretely, it is realized by combining ML classification with entropy-based OOD detection. Finally, the resulting pseudo-labels are used for adaptation by applying a combination of a contrastive and a KL divergence loss. In the extensive experiments, our GMM-based method matched or even improved the current state-of-the-art across all experiments while requiring only a small fraction of the memory necessary for a memory queue or mean teacher.

References

- [1] Mahsa Baktashmotlagh, Masoud Faraki, Tom Drummond, and Mathieu Salzmann. Learning factorized representations for open-set domain adaptation. *arXiv preprint arXiv:1805.12277*, 2018. [2](#)
- [2] Silvia Bucci, Mohammad Reza Loghmani, and Tatiana Tommasi. On the effectiveness of image rotation for open set domain adaptation. In *European conference on computer vision*, pages 422–438. Springer, 2020. [2](#)
- [3] Pau Panareda Busto and Juergen Gall. Open set domain adaptation. In *2017 IEEE International Conference on Computer Vision (ICCV)*, pages 754–763, 2017. [2](#)
- [4] Pau Panareda Busto, Ahsan Iqbal, and Juergen Gall. Open set domain adaptation for image and action recognition. *IEEE transactions on pattern analysis and machine intelligence*, 42(2):413–429, 2018. [2](#)
- [5] Zhangjie Cao, Mingsheng Long, Jianmin Wang, and Michael I Jordan. Partial transfer learning with selective adversarial networks. In *Proceedings of the IEEE conference on computer vision and pattern recognition*, pages 2724–2732, 2018. [2](#)
- [6] Zhangjie Cao, Lijia Ma, Mingsheng Long, and Jianmin Wang. Partial adversarial domain adaptation. In *Proceedings of the European conference on computer vision (ECCV)*, pages 135–150, 2018. [2](#)
- [7] Dian Chen, Dequan Wang, Trevor Darrell, and Sayna Ebrahimi. Contrastive test-time adaptation. In *Proceedings of the IEEE/CVF Conference on Computer Vision and Pattern Recognition (CVPR)*, pages 295–305, June 2022. [1](#), [2](#), [3](#), [6](#)
- [8] Liang Chen, Yihang Lou, Jianzhong He, Tao Bai, and Minghua Deng. Geometric anchor correspondence mining with uncertainty modeling for universal domain adaptation. In *Proceedings of the IEEE/CVF Conference on Computer Vision and Pattern Recognition*, pages 16134–16143, 2022. [2](#)
- [9] Mario Döbler, Robert A Marsden, and Bin Yang. Robust mean teacher for continual and gradual test-time adaptation. In *Proceedings of the IEEE/CVF Conference on Computer Vision and Pattern Recognition*, pages 7704–7714, 2023. [2](#), [3](#)
- [10] Zeyu Feng, Chang Xu, and Dacheng Tao. Open-set hypothesis transfer with semantic consistency. *IEEE Transactions on Image Processing*, 30:6473–6484, 2021. [2](#), [5](#)
- [11] Bo Fu, Zhangjie Cao, Mingsheng Long, and Jianmin Wang. Learning to detect open classes for universal domain adaptation. In *Computer Vision—ECCV 2020: 16th European Conference, Glasgow, UK, August 23–28, 2020, Proceedings, Part XV 16*, pages 567–583. Springer, 2020. [2](#)
- [12] Sachin Goyal, Mingjie Sun, Aditi Raghunathan, and J Zico Kolter. Test time adaptation via conjugate pseudo-labels. *Advances in Neural Information Processing Systems*, 35:6204–6218, 2022. [2](#), [3](#)
- [13] Kaiming He, Xiangyu Zhang, Shaoqing Ren, and Jian Sun. Deep residual learning for image recognition. In *Proceedings of the IEEE conference on computer vision and pattern recognition*, pages 770–778, 2016. [7](#)
- [14] Prannay Khosla, Piotr Teterwak, Chen Wang, Aaron Sarna, Yonglong Tian, Phillip Isola, Aaron Maschiot, Ce Liu, and Dilip Krishnan. Supervised contrastive learning. *Advances in neural information processing systems*, 33:18661–18673, 2020. [5](#)
- [15] Jogendra Nath Kundu, Naveen Venkat, R Venkatesh Babu, et al. Universal source-free domain adaptation. In *Proceedings of the IEEE/CVF Conference on Computer Vision and Pattern Recognition*, pages 4544–4553, 2020. [2](#)
- [16] Jogendra Nath Kundu, Naveen Venkat, Ambareesh Revanur, R Venkatesh Babu, et al. Towards inheritable models for open-set domain adaptation. In *Proceedings of the IEEE/CVF conference on computer vision and pattern recognition*, pages 12376–12385, 2020. [2](#)
- [17] Guangrui Li, Guoliang Kang, Yi Zhu, Yunchao Wei, and Yi Yang. Domain consensus clustering for universal domain adaptation. In *Proceedings of the IEEE/CVF Conference on Computer Vision and Pattern Recognition (CVPR)*, pages 9757–9766, June 2021. [2](#)
- [18] Yushu Li, Xun Xu, Yongyi Su, and Kui Jia. On the robustness of open-world test-time training: Self-training with dynamic prototype expansion. In *Proceedings of the IEEE/CVF International Conference on Computer Vision*, pages 11836–11846, 2023. [2](#), [5](#), [6](#), [7](#), [8](#)
- [19] Jian Liang, Dapeng Hu, and Jiashi Feng. Do we really need to access the source data? source hypothesis transfer for unsupervised domain adaptation. In *Proceedings of the 37th International Conference on Machine Learning, ICML’20*. JMLR.org, 2020. [2](#), [3](#), [7](#)
- [20] Jian Liang, Dapeng Hu, Jiashi Feng, and Ran He. Umad: Universal model adaptation under domain and category shift, 2021. [2](#)
- [21] Tsung-Yi Lin, Michael Maire, Serge Belongie, James Hays, Pietro Perona, Deva Ramanan, Piotr Dollár, and C Lawrence Zitnick. Microsoft coco: Common objects in context. In *Computer Vision—ECCV 2014: 13th European Conference, Zurich, Switzerland, September 6–12, 2014, Proceedings, Part V 13*, pages 740–755. Springer, 2014. [7](#)
- [22] Hong Liu, Zhangjie Cao, Mingsheng Long, Jianmin Wang, and Qiang Yang. Separate to adapt: Open set domain adaptation via progressive separation. In *Proceedings of the IEEE/CVF conference on computer vision and pattern recognition*, pages 2927–2936, 2019. [2](#)
- [23] Xinghong Liu, Yi Zhou, Tao Zhou, Chun-Mei Feng, and Ling Shao. Coca: Classifier-oriented calibration via textual prototype for source-free universal domain adaptation, 2024. [2](#)
- [24] Zhengfa Liu, Guang Chen, Zhijun Li, Yu Kang, Sanqing Qu, and Changjun Jiang. Psdc: A prototype-based shared-dummy classifier model for open-set domain adaptation. *IEEE Transactions on Cybernetics*, pages 1–14, 2022. [2](#)
- [25] Yanzuo Lu, Meng Shen, Andy J Ma, Xiaohua Xie, and Jian-Huang Lai. Mlnet: Mutual learning network with neighborhood invariance for universal domain adaptation, 2024. [2](#)
- [26] Shuaicheng Niu, Jiexiang Wu, Yifan Zhang, Yaofu Chen, Shijian Zheng, Peilin Zhao, and Mingkui Tan. Efficient test-time model adaptation without forgetting. In *Kama-*

- lika Chaudhuri, Stefanie Jegelka, Le Song, Csaba Szepesvari, Gang Niu, and Sivan Sabato, editors, *Proceedings of the 39th International Conference on Machine Learning*, volume 162 of *Proceedings of Machine Learning Research*, pages 16888–16905. PMLR, 17–23 Jul 2022. [2](#)
- [27] Shuaicheng Niu, Jiayang Wu, Yifan Zhang, Zhiquan Wen, Yaofo Chen, Peilin Zhao, and Minghui Tan. Towards stable test-time adaptation in dynamic wild world. *arXiv preprint arXiv:2302.12400*, 2023. [2](#)
- [28] Xingchao Peng, Qinxun Bai, Xide Xia, Zijun Huang, Kate Saenko, and Bo Wang. Moment matching for multi-source domain adaptation. In *Proceedings of the IEEE International Conference on Computer Vision*, pages 1406–1415, 2019. [7](#)
- [29] Xingchao Peng, Ben Usman, Neela Kaushik, Dequan Wang, Judy Hoffman, and Kate Saenko. Visda: A synthetic-to-real benchmark for visual domain adaptation. In *Proceedings of the IEEE Conference on Computer Vision and Pattern Recognition Workshops*, pages 2021–2026, 2018. [7](#)
- [30] Sanqing Qu, Tianpei Zou, Lianghua He, Florian Röhrbein, Alois Knoll, Guang Chen, and Changjun Jiang. Lead: Learning decomposition for source-free universal domain adaptation, 2024. [2](#), [3](#), [7](#), [8](#)
- [31] Sanqing Qu, Tianpei Zou, Florian Röhrbein, Cewu Lu, Guang Chen, Dacheng Tao, and Changjun Jiang. Upcycling models under domain and category shift, 2023. [2](#), [3](#), [7](#), [8](#)
- [32] Sanqing Qu, Tianpei Zou, Florian Röhrbein, Cewu Lu, Guang Chen, Dacheng Tao, and Changjun Jiang. Glc++: Source-free universal domain adaptation through global-local clustering and contrastive affinity learning, 2024. [2](#), [3](#), [7](#), [8](#)
- [33] Joaquin Quionero-Candela, Masashi Sugiyama, Anton Schwaighofer, and Neil D. Lawrence. *Dataset Shift in Machine Learning*. The MIT Press, 2009. [1](#)
- [34] Kuniaki Saito, Donghyun Kim, Stan Sclaroff, and Kate Saenko. Universal domain adaptation through self supervision. *Advances in neural information processing systems*, 33:16282–16292, 2020. [2](#)
- [35] Kuniaki Saito and Kate Saenko. Ovanet: One-vs-all network for universal domain adaptation. In *Proceedings of the IEEE/CVF International Conference on Computer Vision*, pages 9000–9009, 2021. [2](#)
- [36] Kuniaki Saito, Shohei Yamamoto, Yoshitaka Ushiku, and Tatsuya Harada. Open set domain adaptation by backpropagation. In *Proceedings of the European conference on computer vision (ECCV)*, pages 153–168, 2018. [2](#)
- [37] Pascal Schlachter and Bin Yang. Comet: Contrastive mean teacher for online source-free universal domain adaptation. In *International Joint Conference on Neural Networks (IJCNN)*. IEEE, 2024. [1](#), [2](#), [3](#), [5](#), [6](#), [7](#), [8](#)
- [38] Yisheng Song, Ting Wang, Puyu Cai, Subrota K Mondal, and Jyoti Prakash Sahoo. A comprehensive survey of few-shot learning: Evolution, applications, challenges, and opportunities. *ACM Computing Surveys*, 2023. [2](#)
- [39] Dequan Wang, Evan Shelhamer, Shaoteng Liu, Bruno Olshausen, and Trevor Darrell. Tent: Fully test-time adaptation by entropy minimization. In *International Conference on Learning Representations*, 2021. [1](#), [2](#)
- [40] Kaichao You, Mingsheng Long, Zhangjie Cao, Jianmin Wang, and Michael I Jordan. Universal domain adaptation. In *Proceedings of the IEEE/CVF conference on computer vision and pattern recognition*, pages 2720–2729, 2019. [2](#)
- [41] Jing Zhang, Zewei Ding, Wanqing Li, and Philip Ogunbona. Importance weighted adversarial nets for partial domain adaptation. In *Proceedings of the IEEE conference on computer vision and pattern recognition*, pages 8156–8164, 2018. [2](#)
- [42] Da-Wei Zhou, Qi-Wei Wang, Zhi-Hong Qi, Han-Jia Ye, De-Chuan Zhan, and Ziwei Liu. Deep class-incremental learning: A survey, 2023. [2](#)

Supplementary Material

A. Ablation studies

To gain deeper insights into our proposed GMM-based method, we conduct rich ablation studies in the following. Thereby, we use the OPDA scenario on the VisDA-C dataset as a representative example. The OPDA scenario effectively illustrates the challenging trade-off between rejecting new classes and reliably classifying a subset of known classes, while the VisDA-C dataset was selected arbitrarily.

A.1. Contribution of each loss

Fig. 3 illustrates the individual contributions of the contrastive loss \mathcal{L}_C and the KL divergence loss \mathcal{L}_{KLD} to the overall performance of our GMM-based method. Both losses prove to be effective and significantly enhance the source-only performance when used independently. Notably, the KL divergence loss thereby outperforms the contrastive loss, possibly because it impacts both the classifier and the feature extractor, whereas the contrastive loss only optimizes the feature extractor. However, the best results are achieved when combining both losses.

A.2. Hyperparameter sensitivity

To analyze the sensitivity of our GMM-based method to hyperparameter choices, we vary each hyperparameter across a broad range around the chosen value while keeping the others constant. Figs. 4 to 7 show the results. Overall, our approach proves to be robust against these variations which indicates that the choice of hyperparameters is not critical for its success.

Number of dimensions of the reduced feature space:

As shown in Fig. 4, stable performance is maintained when the number of dimensions FD_r of the reduced feature space is above 32. There is minor degradation at $FD_r = 32$ and a significant drop at $FD_r = 16$. Therefore, further reducing the feature space dimensions, e.g. to 48, can enhance memory efficiency without impacting performance.

Rejection rate: Fig. 5 shows that the performance remains nearly constant when varying p_{reject} between 25% and 75%. However, the performance slightly increases with a higher rejection rate. Therefore, discarding more samples during the initialization of τ_k and τ_u can be advantageous.

Number of initialization batches: Similar to FD_r and p_{reject} , the number of batches N_{init} used for initializing τ_k and τ_u does not significantly impact the performance of our method across a broad range of values, as shown in Fig. 6. However, a performance degradation is observed for values smaller than $N_{\text{init}} = 20$. Thus, at least 20 batches are necessary for a representative initialization of τ_k and τ_u .

Batch size: In Fig. 7, we observe that decreasing the batch size starting from 128 only leads to a slight decline in performance until a batch size of 16. However, there is a notable performance drop at a batch size of 8. We suspect this may be due to insufficient initialization of τ_k and τ_u , as N_{init} was kept constant. To test this, we repeated the experiments while adjusting N_{init} to ensure a consistent number of samples for initialization. This adjustment significantly improved performance for a batch size of 8, confirming our hypothesis, while the other results remained constant or showed only a small improvement.

A.3. Ratio of samples used for adaptation

Fig. 8 illustrates how the percentage of samples used for adaptation evolves during the course of an exemplary run. Initially, $p_{\text{reject}} = 50\%$ of samples of the first batch are used for adaptation. During the initialization phase of τ_k and τ_u over the first $N_{\text{init}} = 30$ batches, this percentage remains relatively stable. Post-initialization, the ratio of samples utilized for adaptation steadily increases on average, appearing to converge towards approximately 85%. This trend demonstrates the effectiveness of our adaptation method by showing that the pseudo-labeling becomes increasingly confident over time, resulting in fewer samples being discarded due to uncertainty.

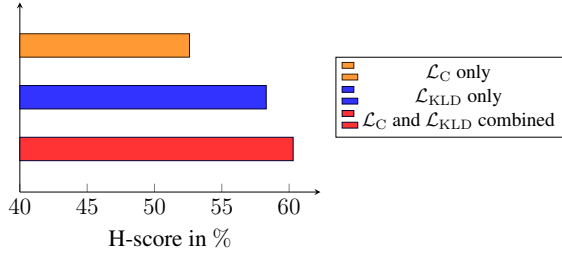


Figure 3. Results using different combinations of the losses \mathcal{L}_C and \mathcal{L}_{KLD} for the VisDA-C OPDA scenario.

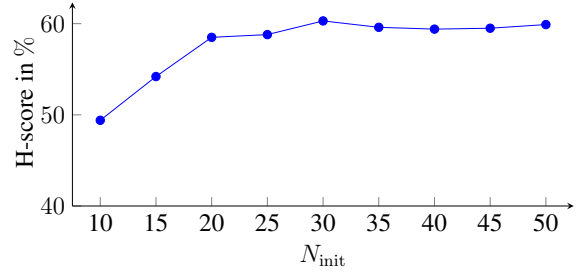


Figure 6. Results for the VisDA-C OPDA scenario using different numbers of batches for the initialization of τ_k and τ_u during pseudo-labeling.

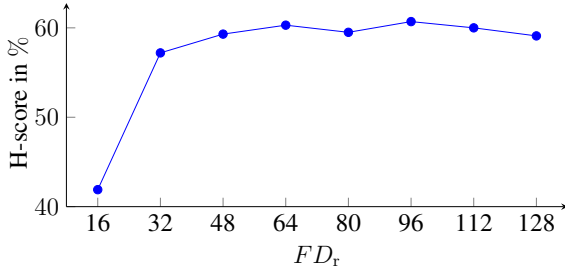


Figure 4. Results for the VisDA-C OPDA scenario using different numbers of dimensions for the reduced feature space.

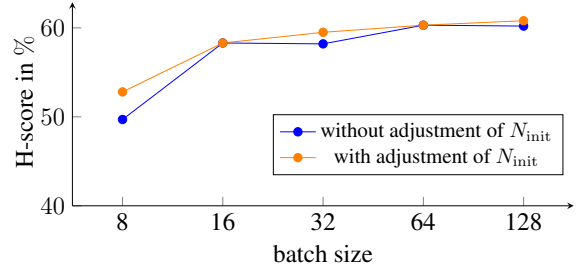


Figure 7. Results for the VisDA-C OPDA scenario using different batch sizes.

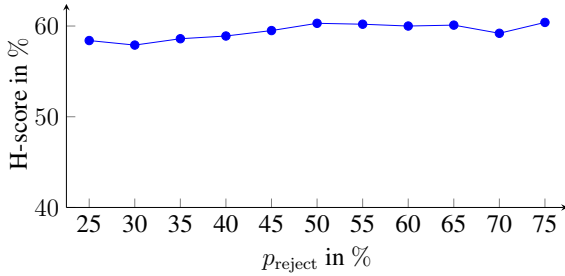


Figure 5. Results for the VisDA-C OPDA scenario using different rejection rates during pseudo-labeling.

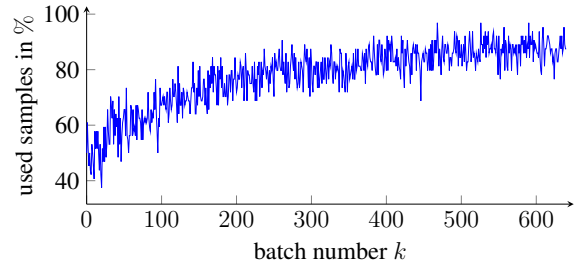


Figure 8. Development of the ratio of samples used for the adaptation over the course of an exemplary run of the VisDA-C OPDA scenario.